ZnS, CdS AND HgS NANOPARTICLES IN POLY(METHYL METHACRYLATE) MATRIX: SYNTHESIS, THERMAL AND STRUCTURAL STUDIES

B. C. EJELONU, P. A. AJIBADE[*]

Department of Chemistry, University of fort Hare, Private Bag X1314, Alice 5700, South Africa.

Zn(II), Cd(II) and Hg(II) complexes of N-hexyl dithiocarbamate was synthesized and characterized using elemental analysis, thermogravimetric analysis; UV-Vis, FTIR and ^{1}H- and ^{13}C-NMR spectroscopy. The metal complexes were thermolysed at 180 °C to prepare hexadecylamine capped metal sulphide nanoparticles and their corresponding metal sulphide nanoparticles/poly(methyl methacrylate) nanocomposites. The optical properties of the nanoparticles and PMMA/nanocomposites were studied by absorption and photoluminescence spectroscopy. The structural studies were carried out with powder X-ray diffraction (PXRD), transmission electron microscopy (TEM), scanning electron microscopy (SEM), energy dispersive X-ray spectroscopy (EDS) and FTIR. The TEM images shows nanoparticles with particles sizes that varied between 3.37-5-89 nm for ZnS and 10.15-37.25 nm for CdS and 9.49-15.60 nm for HgS nanoparticles respectively. The EDS results from the SEM determinations of the different metal sulphide nanoparticles/PMMA nanocomposite materials confirmed the presence of the nanoparticles in the polymer matrix and the broadening of diffraction peaks observed in the XRD of the nanocomposites also confirmed their formation.

1. Introduction

The synthesis of semiconductor metal sulphide nanoparticles have received considerable attention in recent years because of their size dependent properties [1-6]. Group 12 metal dithiolates complexes have taken centre stage in the development of novel single source precursors for the preparation of metal sulphide semiconductor materials [7-10]. Among dithiolates ligands, dithiocarbamate is the most commonly studied especially those derived from alkylamine and the synthesis and characterization of group 12 dithiocarbamate complexes and their use as single source molecular precursors for the synthesis of metal sulphide nanoparticles have been the subject of ongoing research [11-13]. Dithiocarbamate ligands are versatile and possess wide ranging coordination chemistry [14]. They form extremely large number of complexes with transition and non-transition metal ions most of which possess diversified industrial and biological applications [15, 16]. The reduction of the size of materials causes a deviation of their physical and chemical properties from the bulk; and such resultant materials (nanoparticles) are known to possess potential applications and novel properties. ZnS nanoparticles have wide applications in electroluminescence and optoelectronic devices. Among the group II-VI compound materials, it has an energy band gap of 3.68eV; while CdS semiconductor has an energy band gap of 2.5eV and HgS semiconductor (red, distorted rock salt, cinnabar) has a band gap of 2.0eV. The red, distorted rock salt, cinnabar type of HgS semiconductor is said be stable at room temperatures [17-19].

Polymer-inorganic nanocomposites possess greatly enhanced properties and they are of scientific and technological interest because they combine both the properties of the inorganic nanoparticles and the polymer, and generate polymer–inorganic hybrid materials [20, 21]. In

---

[*] Corresponding author: pajibade@ufh.ac.za

continuation of our efforts [22-30] to explore the use of metal chalcogenides, especially dithiocarbamate complexes as single source precursors for the preparation of metal sulphides nanoparticles, we present the synthesis and characterization of hexadecylamine (HDA) capped ZnS, CdS, and HgS nanoparticles/polymethyl methacrylate (PMMA) nanocomposites. The single source precursors were characterized by analytical, spectroscopic and thermal analyses and the optical and structural properties of the resulting metal sulphide nanoparticle/PMMA nanocomposites were studied with optical absorption and emission spectroscopy, powder X-ray diffraction (XRD), transmission electron microscopy (TEM), scanning electron microscopy (SEM) and energy dispersive X-ray spectroscopy (EDS).

2. Experimental

2.1 Materials

Hexamine, aqueous ammonia (15 M) and the respective metal chloride salts- zinc(II) chloride, cadmium(II) chloride and mercury(II) chloride used in this study were all bought from Merck chemicals and were used as obtained without further purification.

2.2 Synthesis of ammonium hexyl dithiocarbamate ligand

The ligand was prepared following a literature procedure [26]. Carbon disulphide (6.00 mL, 0.10 mol) was added into a mixture of hexamine (13.50 mL, 0.10 mol) and 25 mL concentrated aqueous ammonia and stirred for one hour. The white precipitate was washed with diethyl ether and dried in a vacuum. The white ammonium hexyl dithiocarbamate obtained is air and temperature sensitive solid. Yield: 14.58 g (75.15 %).

2.3 Synthesis of the metal complexes

All the metal complexes were prepared following the same method: Hexyl dithiocarbamate (1.25 mmol, 0.243 g) dissolved in 20.00 mL of methanol was added into a 20.00 mL methanol solution of the respective metal salt [$ZnCl_2$ (0.675 mmol, 0.170 g); $CdCl_2$ (0.675 mmol, 0.229 g); $HgCl_2$ (0.675 mmol, 0.339 g)]. The resulting solutions were then stirred for 1 hour; and the solid products obtained for the individual metal complexes were rinsed with distilled water and dried over $CaCl_2$ [26]. The yields of the metal complexes are given as follow: [$(C_6H_{13})NHCS_2ZnS_2CNH(C_6H_{13})$ - {0.36 g; 69.07 %}]; [$(C_6H_{13})NHCS_2CdS_2CNH(C_6H_{13})$ - {0.38g; 66 %}]; and [$(C_6H_{13})NHCS_2HgS_2CNH(C_6H_{13})$ - {0.33 g; 48 %}].

2.4 Synthesis of the metal sulphide nanoparticles

The metal sulphide nanoparticles passivated with hexadecylamine (HDA) were prepared using literature procedure [27]. In a typical synthetic procedure, 0.4 g of each zinc(II), cadmium(II) or mercury(II) complex (ZnL_2; CdL_2; HgL_2) was dissolved in tri-octylphosphine (TOP), followed by the injection of the mixture into 4.0 g of hot HDA at a temperature of 180°C. A fall in temperature was observed (20-30°C); the mixture was allowed to attain the desired temperature again and the refluxing continued for 1 hr after which the mixture was allowed to cool to about 70°C. Methanol was then added to the resultant mixture to remove excess HDA, using centrifugation to separate the flocculent after which the solvent was removed under reduced pressure to obtain the HDA-capped ZnS, CdS, and HgS nanoparticles. The obtained metal sulphide nanoparticles were again washed with methanol three times, filtered and dried at room temperature in the fume cupboard.

2.5 Synthesis of the metal sulphide nanoparticles/PMMA nanocomposites

10.0 mL of toluene containing 0.5 g of polymer (about 3 wt. % of the individual precursors) each was added into three separate glass beakers. Thereafter 10.0 mL of toluene solution containing 0.2 g of the respective metal sulphide nanoparticles was added into each glass beaker, slowly being stirred at first with heating and later vigorously stirred. The polymer dissolved after approximately twenty minutes, and turbid solutions were obtained (white colouration for ZnS nanoparticle, yellow for CdS nanoparticle and faintly blackish colouration for

HgS nanoparticle). The solutions were poured on glass plates and left to dry in air upon which the respective metal sulphide/PMMA nanocomposite materials obtained as powder [31].

2.6 Physical characterization

Elemental analysis was carried out on Perkin Elmer elemental analyzer. The thermogravimetric analysis of the metal complexes was performed using a Perkin Elmer thermogravimetric analyser (TGA 7) fitted with a thermal analysis controller (TAC 7/DX). The FTIR determinations of the metal complexes were done using KBr discs on a Perkin Elmer Paragon 2000 FTIR spectrophotometer in the range 4000-370 cm^{-1}. ^{1}H–NMR and ^{13}C–NMR spectra were obtained on 400 MHz and 101 MHz Bruker NMR spectrophotometers and the electronic spectra was obtained using Perkin Elmer Lambda 25 spectrophotometer in chloroform in the range 800-200 cm^{-1} respectively. Emission spectra of the nanoparticles was determined using Perkin Elmer Lambda 25 spectrophotometer while powder X-ray diffraction patterns of the metal sulphide nanoparticle and metal sulphide nanoparticle-polymer nanocomposites were recorded on a Bruker D8 Advanced, equipped with a proportional counter using Cu Kα radiation (λ=1.5405 A, nickel filter). The scanning electron microscope (SEM) for the nanoparticle and nanocomposite were obtained using JEOL JSM-6390 LVSEM at a rating voltage of 15-20 kV at different magnifications after they were coated with Au/Pd using the Eiko IB.3 Ion coater. Their transmission scanning microscope (TEM) images were obtained on Zeiss Libra 120 (Microscope TEM) using carbon coated copper grids. The FTIR of the PMMA polymer and the metal sulphide PMMA nanocomposites were obtained on a Bruker FTIR Tensor 27 spectrophotometer equipped with silicon ATR.

3. Results and discussion

3.1 Synthesis

The ammonium salt of hexyl dithiocarbamate was synthesized through the reaction of hexamine with carbon disulphide and concentrated aqueous ammonium solution at room temperature. The ligand is air and temperature sensitive. The Zn(II), Cd(II) and Hg(II) complexes were obtained in a substitution reaction between the respective metal chloride salts and the ligand in equimolar ratio. The elemental analysis data showed that the calculated values of carbon, hydrogen and nitrogen are in good agreement with the experimental values (Table 1). The complexes are formulated as four coordinate square planar geometries in which the metal ions are coordinated to two N-hexyl dithiocarbamate ligand acting as bidentate chelating ligand through the sulphur atoms.

Table 1: Elemental analysis of the metal complexes (%)

Metal complexes	Formula weight	Analytical data calculated (Found)		
		Carbon	Hydrogen	Nitrogen
[(C$_6$H$_{13}$)NHCS$_2$ZnS$_2$CNH(C$_6$H$_{13}$)]	418.01	40.23 (39.69)	6.75 (7.04)	6.70 (6.61)
[(C$_6$H$_{13}$)NHCS$_2$CdS$_2$CNH(C$_6$H$_{13}$)]	465.04	36.16 (36.08)	6.07 (6.14)	6.02 (6.01)
[(C$_6$H$_{13}$)NHCS$_2$HgS$_2$CNH(C$_6$H$_{13}$)]	553.22	30.40 (30.57)	5.10 (4.98)	5.06 (4.75)

3.2 Thermal analysis of the complexes

The thermal analyses of the metal complexes was done under nitrogen at a temperature range of 20-800 °C. The degradation patterns of the complexes is presented in Figure 1. Thermal degradation occurred in three steps in the temperature range of 100.5-269.5 °C for the Zn(II) complex; 99.8-270.0 °C for the Cd(II) complex; and 103.1-286.5 °C for the mercury(II) complex. The degradation patterns suggests a gradual decomposition of the metal complexes [32]. At 800 °C, the resulting product of the thermal degradation showed constant mass for Zn and Cd complexes, while for the Hg complex at 425 °C the thermal degradation ended with volatilization of the residue. The result from the thermal analyses of the mercury complex presents the problem of not being able to obtain metal sulphide nanoparticle should the Hg complex be heated beyond 425 °C.
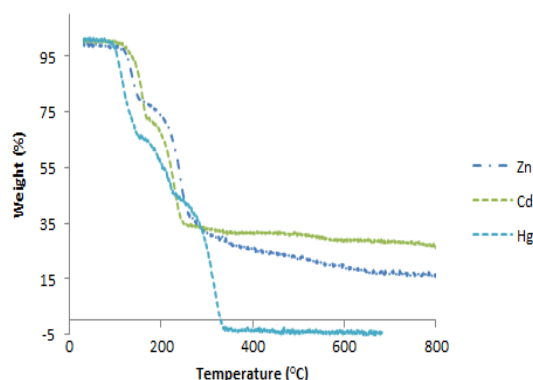

Fig. 1: The overlay thermogravimetric curves of ZnL$_2$, CdL$_2$, and HgL$_2$ complexes

3.3 NMR spectra of the metal complexes

In the ^{1}H-NMR of the metal complexes, the alkyl straight chain signals appear at 0.87, 1.27, 1.36 and 1.32 ppm for the Zn(II) complex, 0.84, 1.25, 1.49 and 2.49 ppm for the Cd complex and 0.86, 1.26, 1.49 and 2.50 ppm for the Hg complex respectively. The N-H protons were observed at 3.45, 3.28 and 3.29 ppm for the Zn(II), Cd(II) and Hg(II) complexes and these values are similar to what is expected from the literature [33, 34]. The ^{13}C-MNR analysis of the complexes revealed six absorption bands each for the respective metal complexes. The methyl-carbon absorbed at 13.95 ppm, 13.88 ppm and 13.80 ppm for $[CH_3-(CH_2)_3-CH_2-CH_2-NHCS_2]_2Zn$, $[CH_3-(CH_2)_3-CH_2-CH_2-NHCS_2]_2Cd$ and $[CH_3-(CH_2)_3-CH_2-CH_2-NHCS_2]_2Hg$ complexes respectively. Each of the methylene groups (CH$_2$) is said to occupy unique environment, and thus giving distinct signals [35]. The methylene groups showed signals at 45.07, 30.98, 29.94, 26.24, and 22.44 ppm for $[CH_3-(CH_2)_3-CH_2-CH_2-NHCS_2]_2Zn$; 40.11, 30.87, 27.71, 25.95 and 21.98 ppm for $[CH_3-(CH_2)_3-CH_2-CH_2-NHCS_2]_2Cd$; and 39.49, 26.91, 25.92, 25.57 and 21.85 ppm for $[CH_3-(CH_2)_3-CH_2-CH_2-NHCS_2]_2Hg$. The CS$_2$ absorption peak for ZnL^2 was observed at 207.24 ppm; 205.43 ppm for CdL^2; and 203.01 ppm for HgL^2 [35].

3.4 Electronic spectra of the metal complexes

Dithiocarbamate complexes give three characteristic absorptions; $\pi \rightarrow \pi^*$ transition of NCS and SCS moieties arising from the chromospheres NS$_2$ and $\pi \rightarrow \pi^*$ transition arising from the transition of an electron of the lone pair electrons on the sulphur atom to an anti-bonding π–orbital [16]. For group 12 metal complexes, the central metal ions possesses pseudo-noble gas electronic configuration (d^{10}), hence no d-d transition over the visible region is expected [16]. The only observed intense bands around 291 nm for the Zn(II), 290 nm for the Cd(II) and 284 nm for the Hg(II) complexes respectively could be attributed to the absorption due to metal to ligands charge transfer transitions (MLCT). [36].

3.5 FTIR spectra studies of the metal complexes

The mode of coordination of alkyl-aryl dithiocarbamate ligands with group 12 metal ions has been reported to be mostly through the sulphur atoms, which appears as single bands often occurring at about 1000 ± 70 [37-39]. In the spectra of bis(hexyldithiocarbamato) complexes of Zn(II), Cd(II) and Hg(II), the coordination of the hexyldithiocarbamate ligand with the metal ions were observed at 953 cm^{-1} for the Zn; 946 cm^{-1} for the Cd and 938 cm^{-1} Hg complexes respectively compared to the band at 931 cm^{-1} in the free ligand. In the FTIR spectra, the presence of CSS band in the free ligand and metal complexes showed that its absorption appeared at relatively higher band for the metal complexes relative to that of the free ligand. The CSS band was observed as a single and strong peak in the order: $ZnL_2 > CdL_2 > HgL_2$. The observed absorption indicates a bidentate coordination of the hexyldithiocarbamate ligand [40].

The υCN stretching frequency of the NCS in the free ligand occurred at 1474 cm^{-1}; and at 1542 cm^{-1}, 1531 cm^{-1}, and 1520 cm^{-1} for the Zn(II), Cd(II), and Hg(II) dithiocarbamate complexes respectively. These results revealed an increase to a higher wave number in the C$\equiv$N absorption band for the metal complexes, this could be ascribed to the delocalization of electron toward the metal centre as a result of the coordination of the ligands to the metal ions [16]. The presence of $\upsilon(CN)$ and $\upsilon(CSS)$ stretching vibration bands confirmed the presence of dithiocarbamate ligand in the metal complexes [41]. The asymmetric alkyl stretching vibration was observed at 2929 cm^{-1} for the free ligand; and appeared at (2930, 2926, and 2929) cm^{-1} for the Zn, Cd and Hg metal complexes respectively. The bands observed at 1327-1343 cm^{-1} are due to the CH bending vibrational modes [26]. The observed N–H stretching bands in the present study are in agreement with the literature value in the region 3300-3500 cm^{-1} [42].

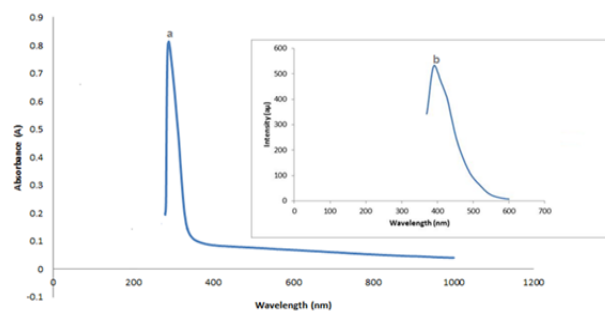### 3.6 Optical and Structural studies of the metal sulphides nanoparticles
3.6.1 Optical properties

Nanoparticles possess reduced size in relation to the excitonic radius of the bulk materials. The presence of excitonic peak or shoulder in nanomaterials is taken as evidence of quantum confinement; and it can be used to estimate its band gap. The band gap of nanocrystalline material has been reported to increase with corresponding reduction in particle size [43]. Figure 2 shows the absorption and emission spectra of ZnS, CdS and HgS nanoparticles. The excitonic peaks are observed to be 289 nm for ZnS; 289 nm for CdS and 292 nm for HgS nanoparticles. The optical absorption maxima of the studied nanoparticles occurred at much more lower wave numbers compared with those of the bulk samples; ZnS = 334 nm; CdS = 516 nm; and HgS = 620 nm. The observed blue shift in the absorption band edges is a consequence of exciton confinement. This is attributed to quantum confinements, confirming a decrease in the size of the particles of the studied nanomaterials. A summary of the band gaps of the different materials arising from their respective absorption maxima is given in Table 2.
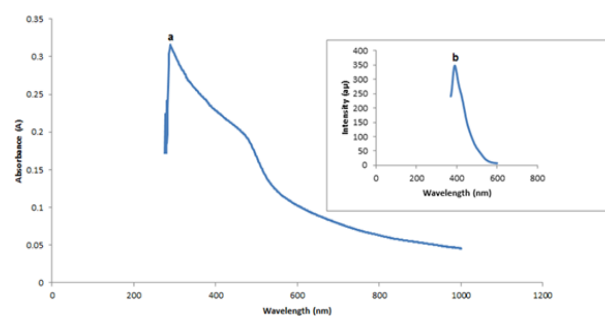
Table 2: The band gaps of the different materials obtained from their absorption maxima

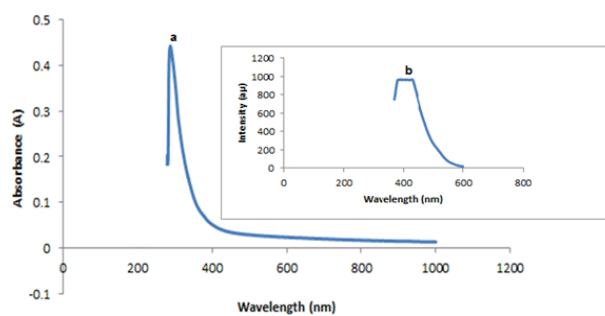| Samples	Samples being Investigated		Bulk Samples	
	Wavelengths (nm)	Band gaps (eV)	Wavelengths (nm)	Band gaps (eV)
ZnS	289	4.29	334	3.71
CdS	289	4.29	516	2.40
HgS	292	4.25	620	2.0

The emission properties of semiconductors nanoparticles have shown that exciton emission is usually observed as sharp band while the trapped emission appears as broad band. These two emission peaks are said to characterize semiconductor nanocrystals emission patterns [27]. In the as-prepared nanoparticles, the emission maxima was observed at 390.5, 388.5 and 428 nm for the ZnS, CdS and HgS nanoparticles respectively. The nanoparticles emission maxima are red-shifted with respect to the absorption edges.

568

(a)

(b)

(c)

Fig. 2. Absorption and emission spectra of the nanoparticles: (a) ZnS; (b) CdS and (c) HgS.

3.6.2 TEM studies of the nanoparticles

The surface morphology and TEM images for ZnS, CdS and HgS nanoparticles are shown in Fig. 3. The SEM images revealed a somewhat spherical shape for ZnS and CdS; and a rod-like shape for HgS nanoparticles respectively, which agglomerated to form larger particles. The TEM micrographs show well-defined nanocrystals for ZnS and CdS. The TEM micrographs also revealed a dot-like- for ZnS, cube-like- for CdS, and spherical- shapes for HgS respectively; and their particle sizes range between 3.37-5.89 nm for ZnS; 10.15-37.25 nm for CdS and for 9.49-15.60 nm HgS nanoparticles respectively [44-46].
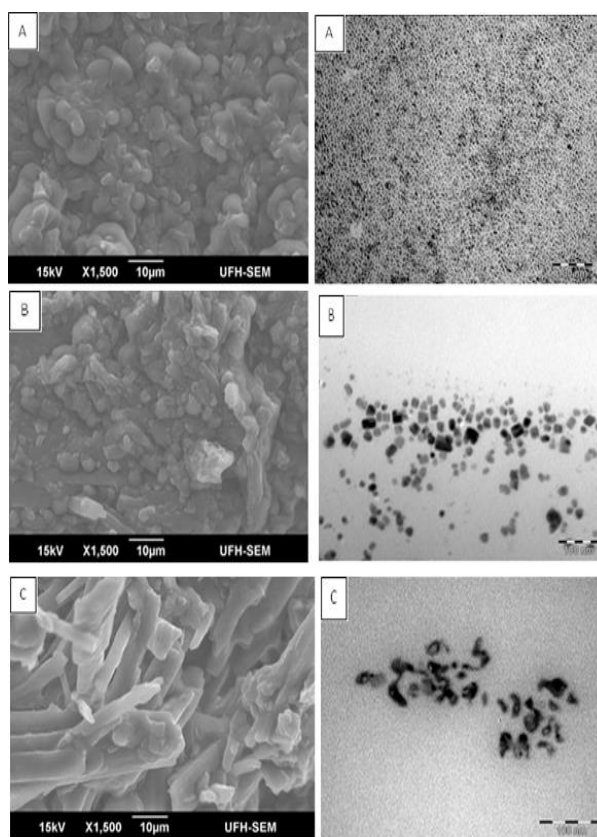
Fig. 3. SEM/TEM images of ZnS (A/A), CdS (B/B) and HgS (C/C) nanoparticles

3.6.3 X-ray diffraction studies

The XRD patterns of the ZnS, CdS and HgS nanoparticles are shown in Figure 4. The broadening of the diffraction peaks for ZnS nanoparticles was observed at $2\theta = 28.05^{\circ}$, 47.89° and 55.87°, which are indexed to (111), (220) and (311) and correspond to the cubic zinc blende structure (JCPDS NO 05-0566) – Figure 4A. The CdS nanoparticles diffraction patterns observed at $2\theta = 27.00^{\circ}$, 32.83°, 44.16° and 52.33° could be indexed to (111), (200), (220) and (311). The observed index numbers of the CdS nanoparticles (Figure 4B) are in agreement with the cubic crystal phase of CdS (JCPDS NO 5-0566). The HgS nanoparticle diffraction patterns were observed at 20.16°, 22.65°, 33.14° and 39.12° indexed to (111), (200), (220) and (311). The XRD patterns (Fig. 4C) are well matched to HgS metacinnabar, syn structure (JCPDS NO 5-0566).

Nanoparticles are known to have higher surface to volume ratio which is said to be important in catalysis [45]. The relatively broader diffraction peaks observed in the ZnS nanoparticles XRD patterns revealed that the ZnS nanoparticles possessed much smaller particle sizes compared to that of CdS and HgS nanoparticles with sharper diffraction peaks suggesting particles of relatively large sizes. The XRD patterns of the metal sulphide nanoparticles are presented in Figure 4. The XRD patterns reveal their nanocrystalline natures, which indicate the broadening of the diffraction peaks due to the higher surface to volume ratio [18]. The nanoparticles sizes were estimated from the corresponding X-ray diffraction peak using Debye-Scherrer's equation [46]. The estimated particle sizes are 9.57 nm for ZnS, 13.21 nm for CdS and 15.95 nm for HgS nanoparticles respectively. The estimated particles sizes are slightly different from those obtained from the TEM micrographs and this could be attributed to the fact that the values obtained from the XRD diffraction patterns are to the best approximation.
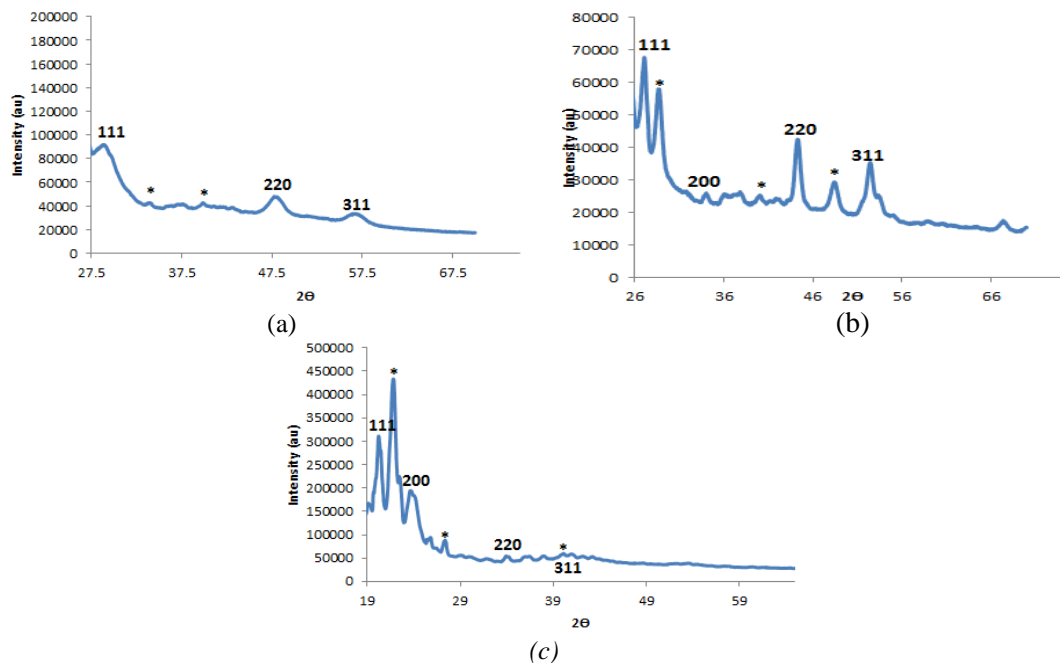
Fig. 4: Powder XRD patterns of ZnS (A); CdS (B) and HgS (C) nanoparticles.
Peaks marked with * are due to HAD

3.7 Morphological studies of the metal sulphide/PMMA nanocomposites

The surface morphology and the level of interface interactions between the ZnS, CdS, and HgS nanoparticles and the organic material (PMMA) were studied using the SEM technique.
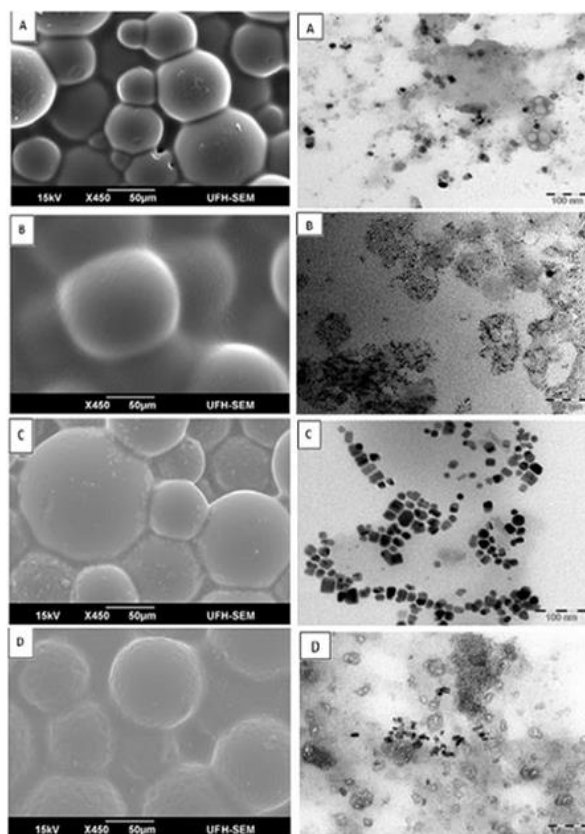

Fig. 5. SEM/TEM images of the respective nanocomposites: PMMA (A); ZnS/PMMA (B/B); CdS/PMMA (C/C) and HgS/PMMA (D/D)

The SEM photographs of the organic material with no nanoparticle added is given in Figure 5A, while those of the metal sulphide nanoparticles with the organic material (ZnS/PMMA; CdS/PMMA and HgS/PMMA) are contained in Figures 5B; 5C and 5D respectively. The SEM images reveal that the particle size for the metal sulphide-organic material (ZnS/PMMA; CdS/PMMA and HgS/PMMA) are relatively enlarged compared to that of the polymer (PMMA) alone, suggesting possible interface interactions between the two (the inorganic and organic materials). The TEM micrographs contained in Figure 5 also show some degree of interactions between the different metal sulphide nanoparticles and the polymer, which allows a combination of properties from the parent constituents into a single material, resulting into new and improved properties [31]. The chemical composition of the metal sulphide/polymer nanocomposites study was carried out with energy dispersive spectroscopy (EDS). The result obtained (Figure 6B – 6D) confirmed the presence of the elemental Zn, Cd, Hg, and S from the ZnS, CdS and HgS nanoparticles.
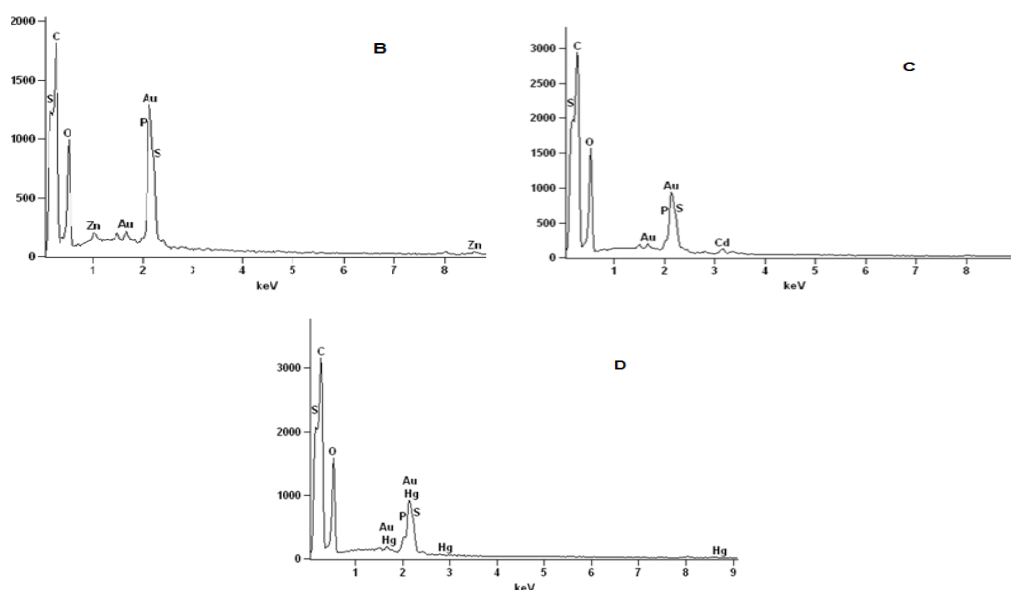

Fig. 6. EDS traces of the respective nanocomposites: ZnS/PMMA (B);
CdS/PMMA (C) and HgS/PMMA (D)

3.8 X-ray diffraction (XRD) patterns of the metal sulphide/PMMA nanocomposites

All the samples analysed show no pronounced differences in their XRD patterns. However, the variations such as little decrease in their respective peak intensities and broadening of diffraction peaks were observed. The observed variations are said to be due to the pore filling effects, suggesting possible reduction in the scattering contrast between the pores and the PPMA. The slight decrease in intensities observed among the samples in moving away from the pure polymer, to ZnS/PMMA, CdS/PMMA, and HgS/PMMA is in agreement with what was observed by Flores-Acosta *et al*. and Sathish *et al*. in their works on zeolites [47, 48]. The X-ray diffraction patterns of the PMMA (without nanoparticle); ZnS/PMMA, CdS/PMMA and HgS/PMMA nanocomposites are presented in Fig. 7.
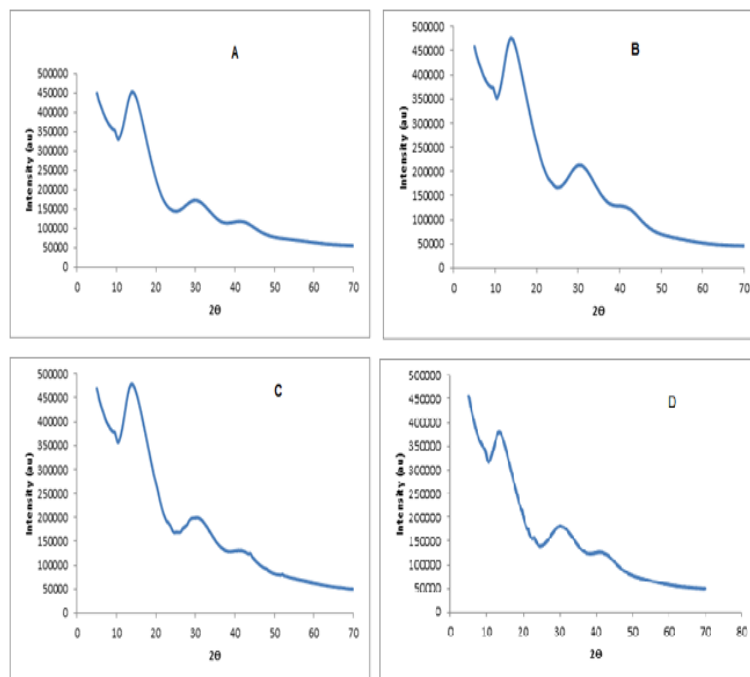
Fig. 7. XRD patterns of the different nanocomposites: PMMA (A); ZnS/PMMA (B); CdS/PMMA (C) and HgS/PMMA (D)

4. Conclusions

Bis(N-hexyl dithiocarbamato) Zn(II), Cd(II) and Hg(II) complexes were synthesized and characterized by elemental analysis and spectroscopic techniques. Their thermal decomposition profiles were studied with thermal gravimetric analysis which confirmed their suitability as precursors for metal sulphides nanoparticles. The metal complexes were used as single source precursors to prepare their respective metal sulphide nanoparticles, as well as their nanocomposites using poly methyl methacrylate (PMMA).

The TEM images shows nanoparticles with particles sizes that varied between 3.37-5-89 nm for ZnS and 10.15-37.25 nm for CdS and 9.49-15.60 nm for HgS nanoparticles respectively. These values differ slightly from the estimated particle size obtained from the XRD diffraction peaks for ZnS, 9.57 nm, for CdS is 13.21 nm and HgS is 15.93 nm. The EDS results from the different metal sulphide nanoparticles/PMMA nanocomposite confirmed the presence of the nanoparticles in the polymer matrix and the broadening of diffraction peaks observed in the XRD of the nanocomposites also confirmed their formation.

References

[1] A.P. Alivisatos, J. Phys. Chem. **100**, 13226 (1996)
[2] C. Burda, X. Chen, R. Narayanan, M.A. El-Sayed, Chem. Rev. **105,** 1025 (2005).
[3] R. S. Friedman, M.C. McAlphine, D.S. Ricketts, D. Ham, C.M. Lieber. Nature

434, 1085 (2005).

[4] G.S. Li, D.Q. Zhang, J.C Yu, Environ. Sci. Technol. **43,** 7079 (2009).

[5] Y. Zhang, N. Zhang, Z.R. Tang, Y.J Xu, Chem. Sci., **3**, 2812 (2012).

[6] N.L. Botha, P.A. Ajibade, Mater. Sci. Semicond. Process. **43**, 149 (2016).

[7] I.J-L. Plante, T.W. Zeid, P. Yang, T. Mokari, J. Mater. Chem. **20**, 6612 (2010).

[8] V.A.V. Schmachtenberg, G. Tontini, J.A. Koch, G.D.L. Semione, V. Drago, J. Phys. Chem. Sol. **87**, 253 (2015).

[9] L.D. Nyamen, V.S.R. Pullabhotla, A.A. Nejo, P. Ndifon, N. Revaprasadu, New J. Chem. **35,** 1133 (2011).

[10] N. Srinivasan, S. Thirumaran, C. R. Chimie, **17,** 964 (2014).

[11] S.R. Trifunovi, Z. Markovi, D. Sladi, K. Andjelkovi, T. Sabo, D. Mini, J. Serb. Chem. Soc. **67**, 115 (2002).

[12] P. O'Brien, R. Nomura, J. Mater. Chem. **5**, 1761 (1995).

[13] N. Adwang, Yousof, N. S. A. M.; Bada, I.; Rajab, N. F.; Hamid, A.; Yamin, B. M.; Halim, A. A. World Appl. Sci. J. **9**(7), 804 (2010).

[14] C. James, D.B. Paul, Dalton Trans. (2007) 1459-1472.

[15] Z.F. Dawood, T.J. Mohammed, M.R. Sharif, Iraqi J. Vet. Sci. **23,** 135 (2009).

[16] P.A. Ajibade, J.Z. Mbese, B. Omondi, Synth. React. Met.-Org. Inorg. Nano- Met Chem. **47**, 202 (2017).

[17] K. Dutta, S. Manna, S.K. De, Syn. Metals. **159**, 315 (2009).

1[8] B. Barman, K.C. Sarma, Optoelectr. Adv. Mater – Rapid Comm. **4,** 1594 (2010).

[19] Gary H. Chemical solution deposition of semiconductor films. Marcel Dekker, Inc 2002, 181.

[20] L. Shanghua, M.L. Meng, S.T. Muhammet, K.K. Do, M. Mamoun, Nano Reviews, **1**, 5214 (2010).

[21] Z. Matusinovic´, M.S. Rogosˇic´, J. Ipusˇic, Poly. Degra. Stability. **94**, 95 (2009).

[22] P.A. Ajibade, J.Z. Mbese, Internat. J. Polym. Sci., **2014**, 1 (2014).

[23] J.Z. Mbese, P.A. Ajibade, Polymers, **6**, 2332 (2014).

[25] J.Z. Mbese, P.A. Ajibade, J. Sulf. Chem., **35**, 438 (2014).

[26] P.A. Ajibade, B.C. Ejelonu, Spectrochim. Acta Part A, **113**, 408 (2013).

[27] T. Chintso, P.A. Ajibade, Mater. Lett. **141**, 1 (2015)

[28] P.A. Ajibade, AC Nqombolo, Chal. Lett, **9**, 498 (2016).

[29] P. A. Ajibade, B.C. Ejelonu, Spectrochim Acta A mol Biomol spectrosc. **113,** 408 (2013).

[30] P.A. Ajibade, N. L. Botha, Results Phys. **6**, 581 (2016).

[31] N. Moloto, N.J. Coville, S.S. Ray, M.J. Moloto, Physica B. **404**, 4461 (2009).

[32] K.S. Siddiqi, S.A.A. Nami, L. Chebude, Y. Chebude, J. Braz. Chem. Soc. **17**, 107 (2006).

[33] V. Alverdi, L. Giovagnini, C. Marzano, R. Seraglia, F. Bettio, S. Sitran, R. Graziani, D. Fregona, J. Inorg. Biochem. **98**, 1117 (2004).

[34] N.F. Kamaludin, N. Awang, I. Baba, A. Hamid, C.K. Meng, Pak. J. Bio. Sci. **16**, 12 (2013).

[35] R. Nomura, A. Takabe, H. Matsuda, Polyhedron **6**, 411 (1987).

[36] C. Y. Su, N. Tang, M. Y. Tan, X. M. Gan, L. P. Cai, Synth. React. Inorg. Met.-Org. Chem., **27,** 291 (1997).

[37] R. A. Gossage, H.A. Jenkins, Acta Chim. Slov. **56**, 329 (2009).

[38] R.A. Howie, E.R.T. Tiekink, J.L. Wardell, S.M.S.V. Wardell, J. Chem. Crystallogr. **39**, 293 (2009).

[39] D. Ondudrušova, M. Pajtášova, E. Jóna, M. Koman, Solid State Phenom. **90-91**, 383 (2003).

[40] J. Osuntokun, P.A. Ajibade, Phys. B, **496**, 106 (2016).

[41] H. Khan, I.S. Butler, A. Badshah, G. Murtaz, M. Said, Z. Rehman, C. Neuhausen, M. Todorova, B. Jean-Claude, Eur. J. Med. Chem. **46**, 4071 (2011).

[42] J. McMurry, Organic Chemisrty, 7th Ed. Thomson Books/Cole, United States. (2008), p. 425.

[43] B. Bochev, G. Yordanov, Colloids Surf. A-Physicochem. Engineer. Aspect. **441**, 84 (2014).

[44] M. Salavati-Niasari, F. Davar, M. Mazaheri, Materials Res. Bull. **44**, 2246 (2009).

[45] A.U. Ubale, S.G. Ibrahim, Inter. J. Mater. Chem. **2**, 57 (2012).

[46] K. Kandasamya, H.B. Singha, S.K. Kulshreshthab, J. Chem. Sci. **121,** 293 (2009).

574

[47] M. Flores-Acostaa, M. Sotelo-Lermac, H. Arizpe-Cha´vez, F.F. Castillo´n-Barrazad, R. Ramı´rez-Bona, Solid State Comm. **128**, 407 (2003).

[48] M. Sathish, B. Viswanathan, R.P. Viswanath, Int. J. Hydr. Ener. **31**, 891 (2006).H. Khan, I.S. Butler, A. Badshah, G. Murtaz, M. Said, Z. Rehman, C. Neuhausen, M. Todorova, B. Jean-Claude, Eur. J. Med. Chem. **46**, 4071 (2011).